

Research Article

Vol. 15, No. 3, 2025, p. 291-304

Impact of Field Characteristics on Pneumatic Seed Drill Performance: A Case Study in Eritrea

T. A. Medhn^{1,2*}, A. G. Levshin², S. G. Teklay¹

1- Department of Agricultural Engineering, Mai-Nefhi College of Engineering and Technology, Eritrea

2- Russian State Agrarian University, Timiryazev Moscow Agricultural Academy, Moscow

(*- Corresponding Author Email: noahtesas@gmail.com)

Received: 27 September 2024

Revised: 14 October 2024

Accepted: 05 November 2024

Available Online: 30 December 2024

How to cite this article:Medhn, T. A., Levshin, A. G., & Teklay, S. G. (2025). Impact of Field Characteristics on Pneumatic Seed Drill Performance: A Case Study in Eritrea. *Journal of Agricultural Machinery*, 15(3), 291-304. <https://doi.org/10.22067/jam.2024.89995.1286>

Abstract

The efficient use of agricultural machinery significantly improves both the quantity and quality of field operations; therefore, it is essential to optimize operational speed and field time. Factors such as field shape complexities and soil surface roughness (SSR) significantly impact seeding performance. The objective of this research was thus to evaluate how these key factors affect seeder performance: (1) field size and shape, and (2) the interaction of seeder speed and SSR. The performance metrics, effective field capacity (F_{eff}), efficiency (η), and average working speed (v_a), were analyzed using SAS software. The convexity (I_{con}) and rectangularity (I_R) indices for each plot were calculated using the ArcGIS minimal bounding geometry Data Management tool, while the elevation standard deviation (σ_e) was computed using Python. The resulting values for F_{eff} , η , and v_a varied widely, with values ranging from 10.2 to 3.1 ha h⁻¹, 30% to 65.7%, and 5.2 to 17 km h⁻¹, respectively. A v_a process capability index (C_{pk}) of 0.22 indicates a significant challenge in meeting the established limits. As the plot run-length increased, the F_{eff} also increased ($R^2 = 42\%$), while it decreased with a rising perimeter to area ratio (P/A) ($R^2 = 51\%$). Additionally, F_{eff} exhibited an upward trend as the I_{con} and I_R indices rose, while it experienced a decline with greater compactness (I_{com}) and square perimeter (I_{sp}) indices; albeit these relationships were not statistically significant. Higher roughness levels generally resulted in a decline in η . Furthermore, operating the planter at higher speed on uneven terrain led to a significant decrease in efficiency. Hence, redesigning the plots to minimize border complexities, eliminating topographic abnormalities, and implementing tailored plot-specific pre-sowing procedures, will significantly enhance planter performance.

Keywords: Effective field capacity, Plots, Shape and size index, Soil surface roughness

Introduction

Mechanizing agricultural systems through the efficient use of machinery unit (MU) (Diao, Takeshima, & Zhang, 2020; Shinde *et al.*, 2023), is a key factor in increasing agricultural production through improving productivity, optimizing operation timing

(such as planting and harvesting), lowering peak labor needs, and minimizing human work drudgery (Srivastava, Goering, & Rohrbach, 2006). MU productivity is measured by the amount of work performed per unit time, which could be the area (ha) processed or the mass of agricultural (crop) product (tonnes) per unit time (Griffel, Vazhnik, Hartley, Hansen, & Richard, 2018; Janulevičius, Šarauskis, Čiplienė, & Juostas, 2019). The area processed per unit time refers to the product of the operational speed (v) and the effective width (w) (Biocca *et al.*, 2022;



©2024 The author(s). This is an open access article distributed under [Creative Commons Attribution 4.0 International License](https://creativecommons.org/licenses/by/4.0/) (CC BY 4.0).

<https://doi.org/10.22067/jam.2024.89995.1286>

Khater, 2017; Zangiev & Skorokhodov, 2018). The MU operational speed is crucial for field operations, particularly for sowing machines, as it affects both the quantity and quality of the output. Research, on sowing quality associated with high speeds, reports operational speed limits due to issues such as excessive lateral soil throws, reduced furrow backfill, and interactions between adjacent furrows (Toscano *et al.*, 2022). Uniform plant stand is achieved by consistent 3D placement of seeds, which necessitates a careful selection of ground speeds (Ale, Manuwa, & Olukunle, 2023; Badua, Sharda, Strasser, & Ciampitti, 2021; Ivančan, Sito, & Fabijanić, 2004; Kirkegaard Nielsen *et al.*, 2018). Variation in sowing depth affects seeds' exposure to moisture and temperature, influencing their germination and survival, which ultimately impacts plant population. Operational speeds higher than optimal limits can result in seeds being planted too shallowly or left uncovered by soil (Brandelero, Adami, Modolo, Baesso, & Fabian, 2015). Operational speed ranges are specific for specific types of planting machines and vary according to the level of technology used. Different literatures claim the minimum, ideal, and maximum limits as 6.5, 8, and 11 km h⁻¹, respectively (Griffel *et al.*, 2018; Janulevičius *et al.*, 2019). It is also reported that pneumatic seeder operating at 10–12 km h⁻¹ provided better uniformity of seed distribution (Toscano *et al.*, 2022), although these parameters are influenced by the physical characteristics of arable soil layer and the texture of the soil surface.

Fields' soil surface texture results from tillage operations could be influenced by various factors, such as moisture content, stoniness of the arable layer, and soil texture. In highly rough fields, planters ought to be operated slower; otherwise, mechanical vibration could be high enough to cause vertical variability (Badua *et al.*, 2021; Wang *et al.*, 2024) in seed placement and exert an influence on seed germination (Kirkegaard Nielsen *et al.*, 2018). Moreover, mechanical vibration causes disassembly of the planter components and increases the risk of minor

and/or major damage; and are also known as significant contributors to musculoskeletal disorders among operators, primarily as a result of whole-body and hand-arm vibrations (Benos, Tsaopoulos, & Bochtis, 2020). Research finding indicated that the shape and size of fields, obstacles, or contour farming usually call for increased maneuverability complications during different field operations (Zangiev & Skorokhodov, 2018). Shape in this study refers to the plot's boundary configurations, including the length and curvature of the perimeters, the presence of obstacles that hinder the navigation of the farm machinery, compactness, convexity of the boundary, and rectangularity. Size, on the other hand, indicates the length of the run and the area of the plot, which usually reduce efficiency by affecting operational speed and productive time moves. The unevenness of the soil surface, subjected to factors such as soil texture, aggregate size, and stoniness, plays a crucial part in planter performances by affecting elements such as lateral and vertical seed placement, operational speed and quality of operation, planter traction, planter stability and maneuverability, and time utilization efficiency. Comprehending the association between soil surface roughness (SSR) and farm machinery performance is indispensable for farm operations' optimization, improving productivity, curtailing in-field operational trials, and helping in decision-making by selecting the type and frequency of operations for specific fields or plots.

Despite the research carried out regarding the influence of field shape and size factors and SSR on the performance of different farm machines, these types of studies have been lacking for Eritrean contexts, particularly for the active wheat sowing implement, the Dora Air Drill. The machinery unit has been operated as per the company's specifications and the operators' experiences. Even though minor changes in field setup and operations can significantly affect machinery productivity, detailed and extensive evaluation of these impacts has been overlooked since the machinery was imported; specifically, the

effects of the field and operational conditions were given little emphasis. Therefore, this research focused on examining how field configuration, soil surface, and topographic conditions interact with operational speed to impact planter performance. It also proposed potential solutions to enhance efficiency.

Materials and Methods

Study Site and MU Description

The research took place at Tselot Farm in Asmara, Eritrea, situated at a Latitude of 15°17'6.4" and a Longitude of 38°56'59", at an altitude of 2341 meters. During the field experiment, the grain drill carried out the usual wheat sowing operations, which covered an area of 107 hectares. The pneumatic and tractor-mounted Nardi Dora Air Drill (DORA 600) with a working width of 6 meters and equipped with 40 coulters was used in this study. For convenient transportation, it can be folded to 2.5 m. The drill was powered by a New Holland T6090 tractor with 152 horsepower. It had Suffolk-style coulters, a standard PTO-driven fan, mechanical bout markers, and an 800-liter hopper, which is standard for all models. The interrow spacing of the drill is 15.3 cm, and it weighs 1090 kg

(AMIA, 2021). Figure 1 shows the elevation map of the site with the plots' polygons (a) and the soil textural class map (b).

A soil texture map of the study area was generated (Fig. 1), showing clay infestation or dominance on one side of the field and loam dominance on the other side. Several plots fell into multiple soil classes, while others fell solely into a single class. Soil texture and composition greatly impact MU performance, with seed drills having different requirements for clayey compared to silty or loamy soils. In clayey soil, the MU requires frequent maintenance due to clogging, leading to prolonged downtime. Additionally, soil texture affects compaction, highlighting the importance of selecting appropriate planters for subsequent operations. Data on soil textural classes were obtained from the national ministry of agriculture for this study.

Despite the variations in soil texture, stoniness, and moisture retention capacity, the type and frequency of tillage operations performed prior to sowing remained consistent. The plots were assumed to be uniform, and tillage frequency, along with the tillage equipment and tractors employed for pre-sowing operations, were similar.

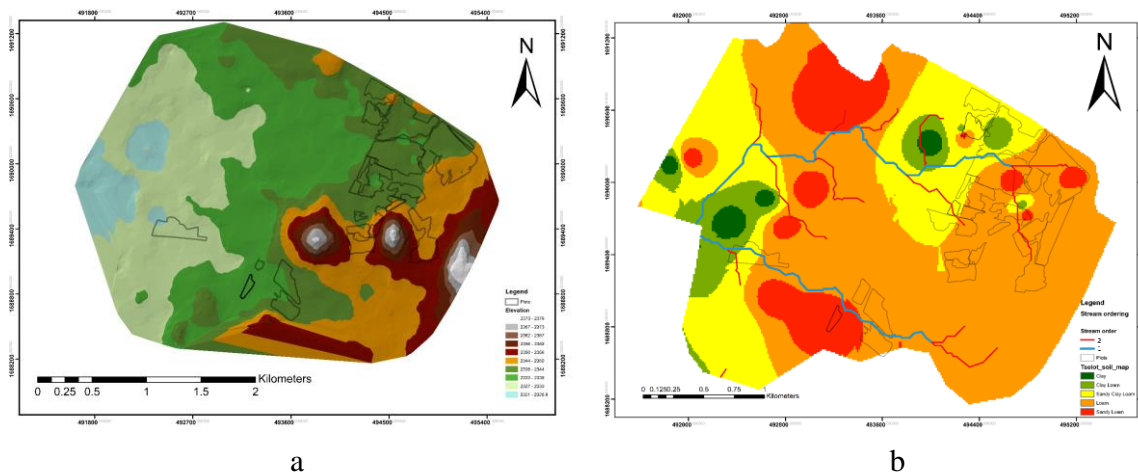


Fig. 1. Study site map showing (a) elevation and the boundaries of the plots, and (b) soil type and stream order

Small drainage channels or sunken areas slow down farm machinery, cause more wear, increase the risk of damaging planter components and requiring more inspections

and adjustments, ultimately increasing downtime. The ModelBuilder tool in ArcGIS—a visual programming language designed for crafting geoprocessing

workflows—was used to automate and detail geographic analysis and data management processes. This tool was utilized for generating the stream orders illustrated in Fig.1b.

Analysis of Planter Performance Parameters

An 8-day experiment was conducted across 23 plots, measuring various metrics, including the time taken for each move by the planter from garage to the field, in the field, and from the field back to the garage. The recorded on-farm operations include the main working time, idle travel time, and periods of downtime, along with spatial details that contribute to the study.

To assess the performance of the planter, the parameters considered were the effective field capacity (F_{eff}), efficiency (η), and average working speed (v_a), which were determined by expressions 1, 2, and 3, respectively (Janulevičius *et al.*, 2019; Srivastava *et al.*, 2006; Toba, Griffel, & Hartley, 2020; Zangiev & Skorokhodov, 2018).

$$F_{eff} = \frac{A}{T_{total}} \quad (1)$$

$$\eta = \frac{T_1}{T_k} = \frac{\sum_{i=1}^n t_n}{\sum_{i=1}^k t_k} \quad (2)$$

$$v_a = \frac{A}{T_1} \times \frac{10}{w} \quad (3)$$

where $A = \sum_1^k a_k \Rightarrow a_k = l_n \times w$; a_k —the actual processed area in pass ‘ k ’, ha ; T_{total} —the total time taken to complete the plot, s ; l_n —length of the working pass ‘ n ’, m ; t_n —working pass time, s ; t_k —time taken to complete pass ‘ k ’, s (time taken from the start of pass ‘ k ’ to the start of pass $k+1$). The t_k includes the working pass time and overhead time (time taken for turning, technical adjustment, seed hopper checking, etc.); and w —working pass width ($w = 6.15$ m for the specified planter) (Oksanen, 2013; Vereshchagin *et al.*, 2018).

The v_a was assessed for its capability to remain within predefined operating limits as documented in literature, which can be done via process capability test. Process capability is used to quantify the ability of a manufacturing process to meet standard or user-defined specifications. In other words, it

assesses a process’s capability to operate within predefined limits and levels of precision, thereby verifying its ability to meet the specified requirements. Process capability indices are often used in the domains of statistical quality control and process control, serving as vital tools to assess the efficiency and effectiveness of manufacturing processes. This approach, using SAS software, was adopted to ensure compliance of v_a with the specified limits. In this study, the planter’s operational speed was tested to determine its capability to meet specified requirements and to evaluate the quality of its performance in relation to the ability test.

The following four categories are widely recognized as fundamental measures of process capability indicators (Matsuura, 2023; Montgomery, 2013; Wu, Pearn, & Kotz, 2009).

$$C_p = \frac{USL - LSL}{6\sigma} \quad (4)$$

$$C_{pL} = \frac{\mu - LSL}{6\sigma} \quad (5)$$

$$C_{pU} = \frac{USL - \mu}{6\sigma} \quad (6)$$

$$C_{pk} = \min \{C_{pU}; C_{pL}\} \quad (7)$$

where C_p is the process capability index; C_{pL} and C_{pU} are the lower and upper process capability indices, respectively; μ is the process mean; σ is the process standard deviation; LSL is the lower specification limit; and USL is the upper specification limit. $C_p < 1$ indicates that speed of operation is not well centered (process incapable), meaning that the speed of operation often exceeds the specification limits; $C_p = 1$ indicates the variability of the speed of operation is the same as the specification, but there is no margin for errors; and $C_p > 1$ ensures better performance, denoting the speed of operation does not exceed the USL or fall below the LSL, with a higher value demonstrating higher capability.

Equation 4 indicates the degree to which speed variation fits within the specification limits. A higher value reflects a narrower speed spread in relation to these limits, signifying enhanced capability. Whereas

Equations 5 and 6 evaluate the speed capability by comparing the mean speed to the lower and upper specification limits (LSL and USL), considering the speed variability. C_{pk} (Equation 7) compares both the LSL and USL to assess overall capability. A C_{pk} value greater than 1 indicates that the process speed meets or exceeds the specified requirements.

Factors that Influence the Performance of a Planter

Field conditions: layout and dimension of field polygons, soil texture, terrain slope, soil moisture, obstacles, and rough surfaces; and **operational parameters:** consistent maintenance to diminish downtime and the skill level of the operator are vital factors for planter performance. A thorough investigation of the interplay between field conditions and operational factors is essential for enhancing planter performance, as it reveals adaptable solutions that can be implemented effectively.

Shape and Size Indices

A plot in this article describes a two-dimensional area that might contain natural and man-made obstacles like holes, stone piles, and electric poles as subsets. This article presents metrics for 23 plots, focusing on the following indices: average plot run length, convexity (I_{con}), perimeter to area ratio (P/A), compactness index (I_{com}), square-perimeter index (I_{sp}), and rectangularity (I_r) (Demetriou, See, & Stillwell, 2013; Griffel et al., 2018; Oksanen, 2013). The brief descriptions of

these indices are as follows:

The smallest convex polygon encompassing all the vertices of a given polygon is known as a convex hull. A_{coh} being the convex hull area (Fig. 2b), I_{con} can be determined by Equation 8. Similarly, shape complexity can be quantified by the relationship between the perimeter (P) and the area of the shape, and it provides important information on the complexity and irregularity of a polygon employing the length of the boundary relative to the enclosed area (Equation 9). When calculating the perimeter of plots, those with highly broken and jagged boundaries are referred to as irregular or complex boundary plots.

$$I_{con} = \frac{A}{A_{coh}} \quad (8)$$

$$P - A_{ratio} = \frac{P}{A} \quad (9)$$

Compactness measures how circular a polygon is and is given by Equation 10, while the square perimeter index represents the relationship between the square root of the area and the polygon's perimeter (Equation 11).

$$I_{com} = 4\pi \frac{A}{P^2} \quad (10)$$

$$I_{sp} = \frac{4\sqrt{A}}{P} \quad (11)$$

Rectangular fields are preferred in agriculture because they allow for straight, parallel swaths, making them more convenient to manage unless specific needs arise.

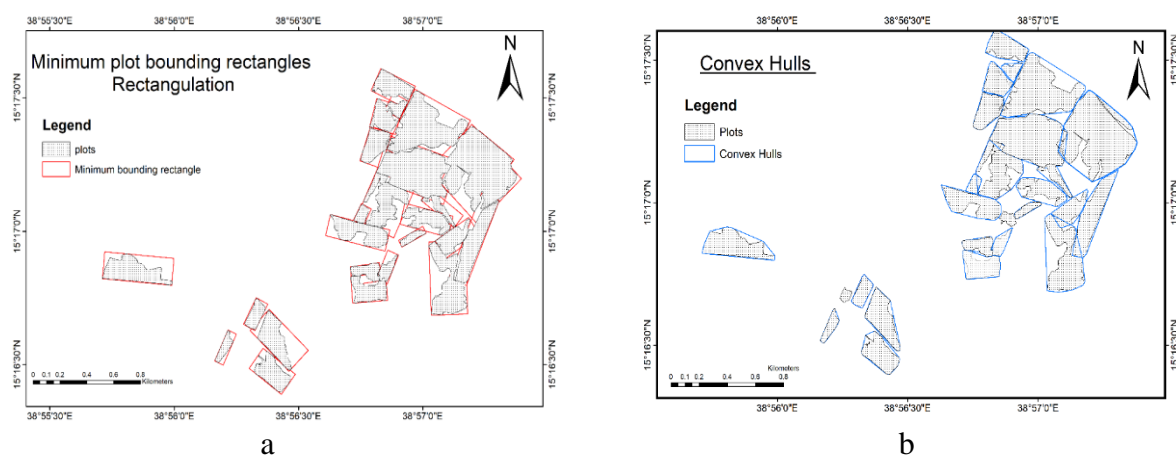


Fig. 2. (a) Minimum bounding rectangles and (b) convex hulls results of ArcGIS

The area of a minimum bounding rectangle (A_{mbr}) (Fig. 2a) is considered to define the rectangularity index, Equation 12.

$$I_r = \frac{A}{A_{mbr}} \quad (12)$$

The areas of the convex hull and minimum bounding rectangle for each plot were computed with the assistance of the ArcGIS tool. The Locus GIS offline land survey—offline data collector, mapper, area calculator, and SHP editor version 1.17.0—was used to calculate the area of individual plots, determine field boundaries, and track the routes for specific plots. Google Earth Pro and ArcGIS tools were utilized for further processing. The areas calculated by the mobile application were verified with the areas calculated by Garmin GPS, and the areas obtained by digitizing the margins of individual plots in Google Earth Pro; and were found to be reliable for use.

Soil Surface Roughness Analysis

The elevation standard deviation was employed in determining the SSR index in this research, which comprises determination of the standard deviation of elevations (σ_e) (Equation 13) (Herodowicz-Mleczak, Piekarczyk, Kaźmierowski, Nowosad, & Mleczak, 2022) across the surface of the plots. A higher σ_e implies substantial variability and intricacy in soil surface elevation.

$$\sigma_e = \left(\frac{\sum_{i=1}^n (Z_i - Z_{ref})^2}{n-1} \right)^{\frac{1}{2}} \quad (13)$$

where Z_i —elevation (m) reading above mean sea level at location i ; Z_{ref} —reference elevation; and n —number of elevation readings.

Data was analyzed using the Python programming language within the Anaconda distribution environment, utilizing Pandas for data manipulation, NumPy for numerical operations, and SciPy's ndimage module for image processing functions.

Results and Discussion

Analysis of Planter Performance Parameters

Field efficiency, effective field capacity, and average operational speed appear to be the

top measures for assessing a planter's performance. Typically, planters' η ranges between 55 and 80%, with 70% being ideal (Srivastava *et al.*, 2006). The v_a limits are 5, 8, and 12 km h⁻¹ (Srivastava *et al.*, 2006; Toscano *et al.*, 2022). The η (%) and v_a (km h⁻¹) lie in the range of 30–65.7% and 5.2–17 km h⁻¹, respectively. Generally, η is much lower than the typical ranges; 70% fall below the lower limit of the range, 30% between the lower and typical values, and there are no values exceeding the typical value.

The v_a capability test assessed v_a 's ability to adhere to acceptable speed limits. For this test, the acceptable speed limits are defined by the LPS, target, and USL. As illustrated in Fig. 3, the speed data was tested for distribution and capability, and a lognormal distribution model found the best model with AIC, AIC Weight, and BIC values of 121.3, 0.4, and 123, respectively. The test results showed a mean of 10.32, a standard deviation of 3.37, and a coefficient of variation (CV) of 32.64%. This signifies higher variability of v_a , which could have contributed to the reduction and variation in η and F_{eff} . According to Equation 7, C_{pk} was 0.22, indicating that the planter v_a was not good enough to optimally adhere to the specified limits, as a lower value indicates a weakness in the process (Matsuura, 2023). The v_a had 28% off-range values, with 2% below the LSL and 26% above the USL. Additionally, 83% of the v_a exceed the USL, corresponding to efficiencies less than 45%; 10% less than the lower efficiency limit indicated. This suggested that the increased v_a in the region higher than the USL was accompanied by a severe reduction in η .

The specified planter has a constant constructional width of 6 m, which means F_{eff} and v_a are directly related (Fig. 4). This relationship shows that both are negatively correlated with η ($R^2 = -0.48$), indicating that as the v_a increases, η tends to decrease. This suggests that an increase in v_a leads to a reduction of η and the planter's performance.

Intricate the maneuverability, leading operators to favor slower driving speeds and operate at variable speeds for greater control.

Consequently, increased complexity in plot boundary is accompanied by lower planter performance.

Furthermore, the correlation coefficient of 0.41 illustrates that F_{eff} responded moderately to the length variability of the plots (run length). The association is statistically

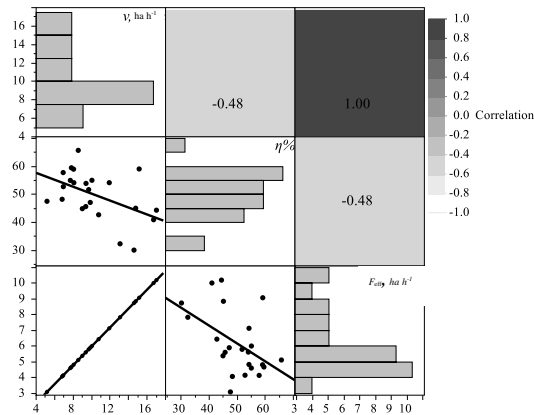


Fig.3. Correlation matrix of the length of the plots, efficiency, effective filed capacity, and operational speed

The negative correlation serves as a warning alert for planter operators and farm managers, emphasizing the importance of balancing the increase in v_a while ensuring the retention of optimal η levels. Because, as indicated in Fig. 3, higher v_a can improve planter productivity, but it may also lead to a reduced η due to issues such as equipment wear, decreased precision, and increased energy consumption. Comprehending the relationship could help operators make informed decisions and adjust operational parameters to maximize productivity while optimizing efficiency. Increased fuel consumption could result in higher emissions, impacting environmental sustainability.

Effect of Shape and Size Indices on the Effective Field Capacity

This section discusses the correlation between size and shape indices and the effective field capacity, with results presented in Fig. 5. The P/A showed a moderately strong correlation with F_{eff} , indicating that 51% of the variability in F_{eff} can be accounted for by the changes in P/A. F_{eff} decreased as the P/A rose at a decreasing rate. A higher P/A signifies a more intricate and irregular boundary,

signifying a moderate association, although only 41% of the change in the F_{eff} can be explained by the average length of the plots, suggesting the relationship is not robust enough to promise a perfect connection. As the average plot length increased, the F_{eff} also increased at a decreasing rate.

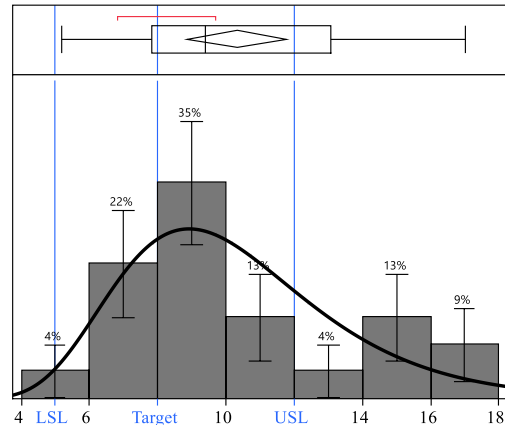


Fig.4. Speed distribution and specification limits

resulting in an increase in the P/A value. As depicted in Fig. 5, the P/A has the highest correlation, implying that this shape index has the greatest impact on the F_{eff} . Because the more complicated the boundary, the more

Analytically, the F_{eff} can be explained as the product of η , v_a , and w , with v_a being directly proportional to the run-length of the plot. Based on this relationship, the maximum length would be expected to result in maximum F_{eff} ; however, due to the variation in downtimes, longer plots did not necessarily correspond to higher F_{eff} . In practice, longer plots need a smaller number of turnings than shorter plots with the same area, which ideally, is expected to have a higher η . However, the η appeared to be uncorrelated with the run-length. This could be due to the increased time required for repair and inspection at the headlands as a result of repeated disassembling of the functional components of the planter caused by the v_a exceeding the USL. The situation led to higher mechanical vibrations, especially in relatively rough areas. This part is detailed in Section 3.3, as it could have a relationship with mechanical vibration in relation to higher speeds.

F_{eff} also tended to increase with the increase in I_{con} and I_R and decrease with I_{com} and I_{sp} , although the correlations were not significant. I_R , I_{con} , I_{com} , and I_{sp} evinced feeble relationships with the F_{eff} (Fig. 5), implying weaker influence on the performance of the

machine. Furthermore, the 26% exceedances of the v_a beyond the USL is an indication that the planter was frequently operated outside the permissible v_a limits, which could lead to suboptimal performance and potential quality reduction.

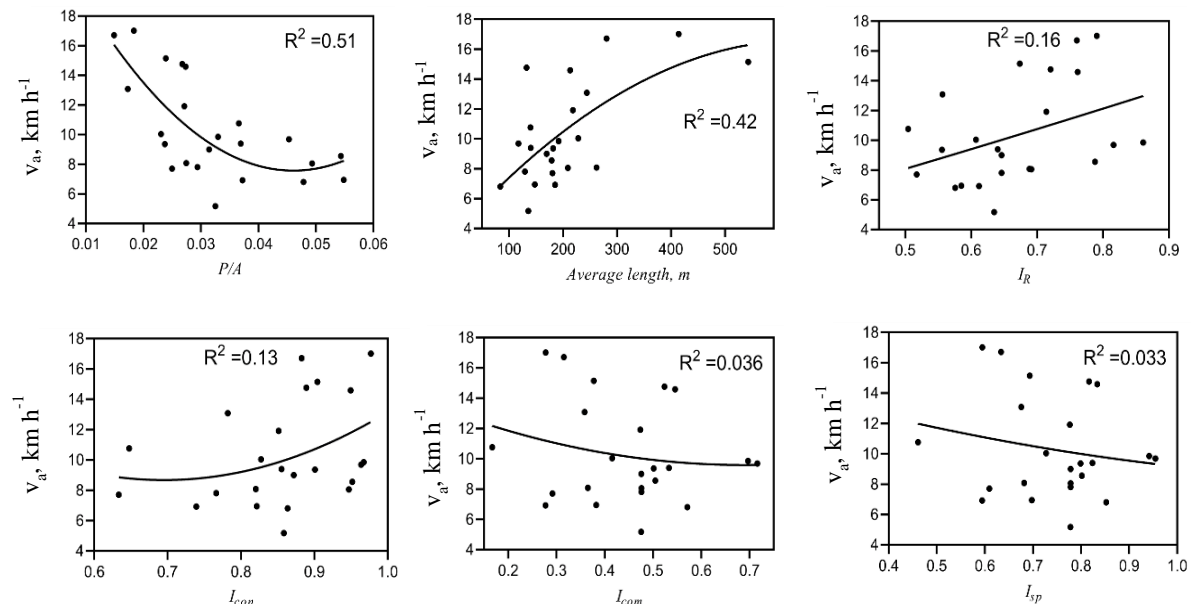


Fig. 5. Correlation between effective average speed and shape and size indices

This might lead to the variability of seed placement in three dimensions: vertically below the soil surface, horizontally along the rows, and across the swath. Variability in seed exposure to moisture and temperature can cause differences in germination, leading to variations in plant population density. Similar research has also reported that higher speeds cause issues with quality of operation and productivity (Brandelero *et al.*, 2015).

Soil Surface Roughness Analysis

The difference in soil moisture content and texture exhibited varying responses to tillage, resulting in inconsistency in surface. This led to cloddy or fine tillage outputs depending on specific conditions. Figure 6 (a and b) were taken from proximity of the same field but exhibit differences in surface textures, while those in Fig. 6 (c and d) – a few hundred meters apart, exhibited different soil classes and different surface finishes.

For better visualization of the plots'

topographic variation and irregularity, the difference of the surface elevations and the mean plot elevations were 3D-plotted in Fig. 7 using Python programming. This figure represents the peaks and nadirs of the plots which the planter had passed over in performing the operations. As illustrated, the plots are uneven, requiring the planter to frequently ascent and descend over short distances in some areas. Other plots are sloping, which could complicate maneuverability and impose lateral instability issues on the planter functional components. These inconveniences slowed down the operational speed, impacted F_{eff} , and contributed to the variation in the performance of the planter. Moreover, the drainage channels of varying stream orders illustrated in Fig. 1 were also an addition to the roughness complications. Plots 4, 6, 9, 10.1, and 11 are crossed by shallow natural drainage channels of 2nd-order streams, while 2 and 13 are crossed by 1st-order streams. These drainage

channels added complications to the topography and intricate field operation (Fig. 7), making maneuverability difficult and affecting the speed of operation. The drainage channels are naturally oriented in such a manner that the planters must cross them over considerably larger areas of the plot. This

required the operator to frequently change gears to regulate the speed when approaching and receding the channels. Therefore, the planter had to decelerate when approaching the drainage channels and nadirs or peaks and then accelerate, which contributed to the speed variability and, therefore, to the performance.

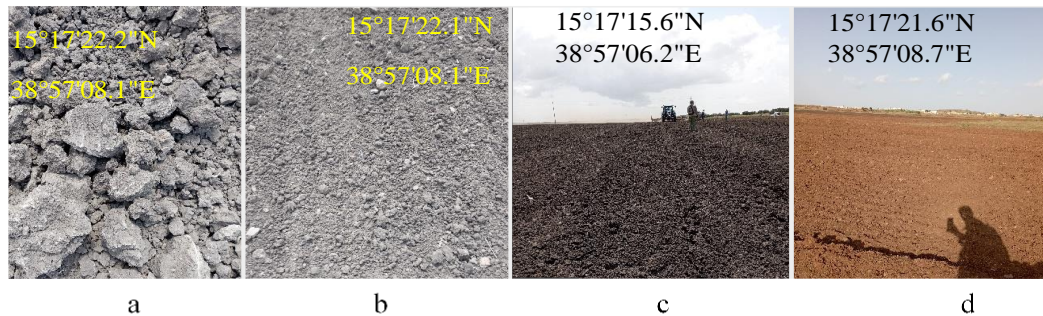


Fig. 6. Variations in Surface Textures and Soil Classes: (a) and (b) showing differing surface textures observed within the same plot; (c) and (d), taken a few hundred meters apart, highlight distinct soil classes and surface finishes.

The impact of SSR on the planter performance parameters was analyzed employing the elevation standard deviation (σ_e) as a measure of roughness index. Based on this, the plots were classified into 3 categories shown in Table 1: high (highest 25%), moderate (middle 50%), and low roughness (lowest 25%).

In this section, the analysis was conducted in two stages: initially, the trend of the η was analyzed against the overall patterns of the SSR. Then individual category analysis took place to compare the η among the SSR categories and examine the trend within each category in relation to the SSR and v_a ,

analytically. This part considered extreme values of v_a , i.e., above the USL, in relation to the σ value in general and the higher values of σ_e in particular.

The overall trend of the η in relation to the holistic SSR indices is depicted in Fig. 8a. As plot10.5 is small (0.8 ha) and the η of the planter is exclusively higher than the second highest η by around 7%, it is excluded from the analysis given in Fig. 8a for better visualization. The η has shown a decreasing trend as σ_e increased, with correlation coefficients of 0.24. This indicates that η responded relatively mildly to the overall SSR.

Table 1- Elevation (above mean sea level) standard deviation as a measure of SSR index

Low roughness index					Medium roughness index					High roughness index				
Plot name*	σ_e	v_a	$\eta\%$	F_{eff}	Plot name*	σ_e	v_a	$\eta\%$	F_{eff}	Plot name*	σ_e	v_a	$\eta\%$	F_{eff}
12.4	0.20	8.1	59.0	4.8	10.1	0.99	8.1	54.2	4.8	12.3	1.56	11.9	54.2	7.1
8A'	0.49	6.8	48.3	4.1	13	0.99	10.0	55.0	6.0	2	1.56	17	44.4	10.2
6	0.50	9.0	44.9	5.4	7A	1.03	6.9	57.8	4.2	11	1.65	9.4	53.9	5.6
9	0.57	9.7	51.7	5.8	10.3	1.14	7.8	59.5	4.7	1	1.79	14.6	30.1	8.8
10.7	0.83	7.7	55.0	4.6	5	1.25	15.1	59.1	9.1	10.5	2.44	8.6	65.7	5.1
10.4	0.96	6.9	52.8	4.2	8A	1.29	5.2	47.5	3.1	4	2.65	16.7	41	10
					12.2	1.30	9.4	45.7	5.6					
					12.1	1.35	9.9	47.1	5.9					
					7(B+C)	1.41	10.8	42.7	6.5					
					8B	1.49	14.8	45.1	8.9					
					3	1.54	13.1	32.4	7.8					
Average $\eta\% = 51.9$					Average $\eta\% = 49.6$					Average $\eta\% = 48.2$				

*Plot name column should be read as plotx, for example, a plot name indicating 12.4 is the same as plot12.4.

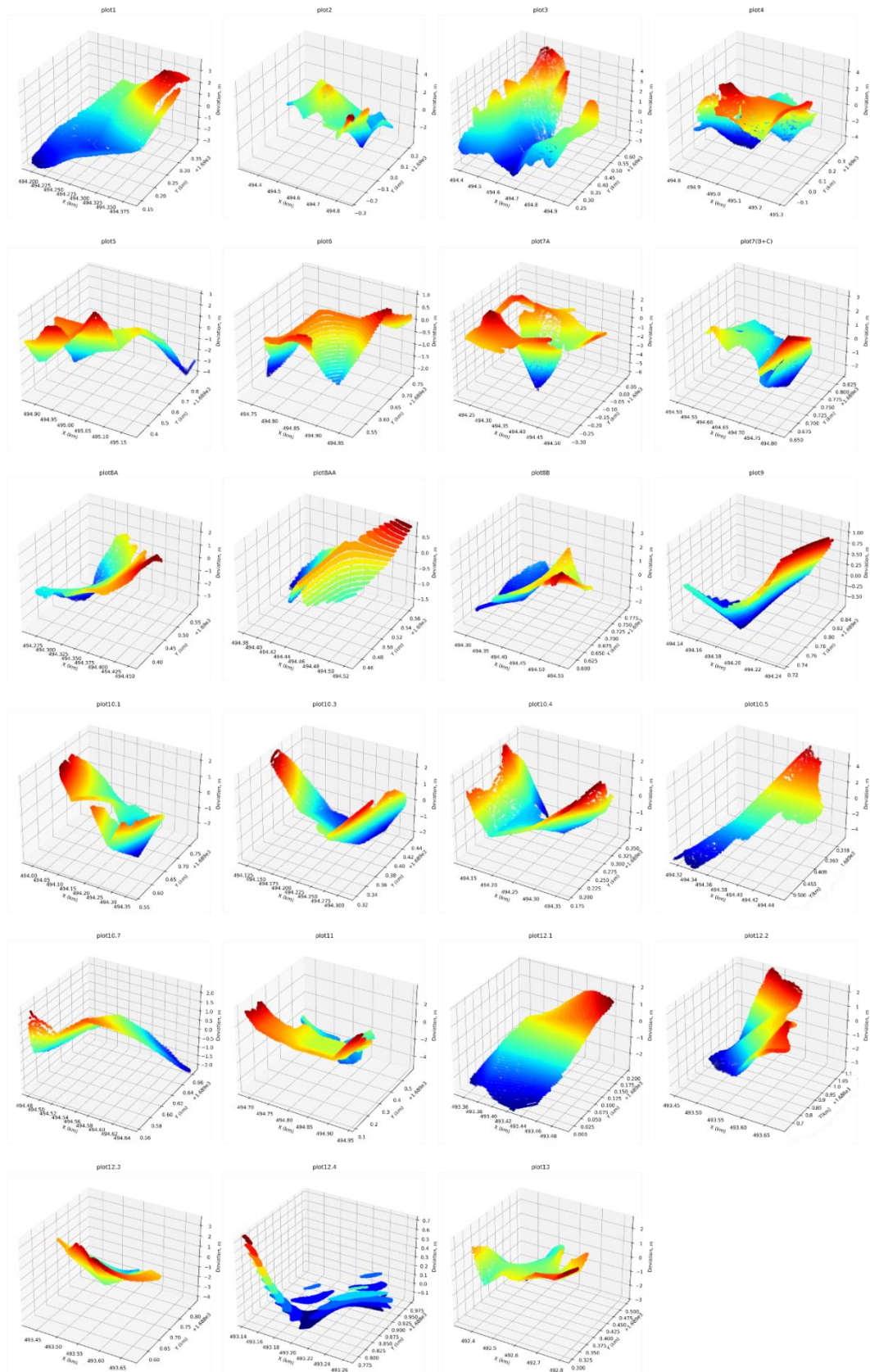


Fig. 7. Plots' topographic variation and irregularity, generated from the deviation of the surface elevation from the mean plot elevation

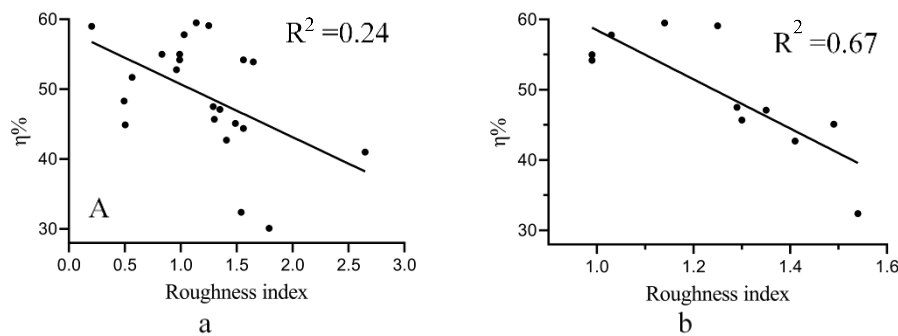


Fig. 8. Relationship between η and σ_e for (a) the 22 plots and (b) the plots with moderate roughness

As shown in Table 1, the average $\eta\%$ decreased as the roughness category increased, i.e., the average η for the lower, moderate, and high roughness categories were 51.9%, 49.6%, and 48.2%, respectively.

Low roughness category: The v_a was within the allowable limit in all the plots; the shorter length of the plots seems to have hindered the operator from accelerating as fast as they could have on longer plots. The η showed a mild trend with the increase in roughness index (Table 1).

Moderate roughness category: This data represents 50% of the total plots, and a correlation graph was created to visualize the relationship between η and the roughness index (Fig. 8b). As the SSR increased, the η decreased, with a correlation coefficient of 0.67, indicating a strong and consistent relationship. This demonstrates that 67% of the variability in η can be characterized by SSR variability. In other words, the SSR did have a strong influence on machinery performance. As the roughness increased (for instance, due to roughened terrain and soil surface texture), the η decreased in at least half of the plots. Therefore, as the SSR increases, planters may experience a decrease in performance.

High roughness category: Generally, in this category, as the planter v_a exceeded the USL, the η was diminished (plot names: plot1, plot2, and plot4). Additionally, operations at high SSR and higher speed are characterized by reduced η (plot1 and plot4 in Table 1). Thus, when the planter was operated at v_a higher than the USL and the soil surface was

rougher, the η values were among the lowest.

Therefore, based on the complex interaction between SSR and η , planters operated in smoother soils complying with the operational constraints can effectively be exploited without being influenced by the soil roughness conditions. However, as soil roughness increased to a moderate level, the planter performance became more sensitive to the soil roughness variability, impacting the planter performance explicitly. This could be due to the increase in mechanical vibrations that lead to temporary dismantling of the planter components or damage to parts sensitive to mechanical vibrations, ultimately increasing downtime. At the highest SSR category, however, the combined effect of the interplay between high SSR and exceedance of the average operational speed from the USL excessively challenged the machinery performance, resulting in low efficiency. Thus, farm managers and machinery operators could comprehend these dynamics and develop focused techniques to maximize machinery performance in different soil conditions to pursue improved productivity and longevity in farm operations.

Conclusion

This study found that the performance of a seeder is significantly influenced by plot length, boundary complications, and soil roughness. Longer, rectangular plots generally enhance seeder performance by minimizing idle travels and reducing variability in operational parameters. As plot area to

perimeter ratio (P/A) increases, the effective field capacity decreases.

Soil roughness also plays a crucial role, with efficiency decreasing as roughness increases. Operating machinery at high speeds on rough terrain notably reduces efficiency. Therefore, field levelling to remove irregularities is a prime requirement. Pre-sowing tillage operations should be tailored to specific fields for better output.

The study concludes that the combined effect of field boundary layouts and soil surface roughness significantly reduces machinery performance. Hence, these factors need careful consideration in optimizing farm machinery operations. Other plot-specific factors, such as impediments, soil moisture content, and operator conditions, which were not extensively covered in this study, also need to be considered for maximizing productivity.

Understanding the impact of off-range speeds can help farm managers and operators optimize efficiency and minimize downtime.

Conflict of Interest: The authors declare no competing interests.

Authors Contribution

Tesfit A. Medhn: Responsible for conceptualization, Study design, Data collection, Methodology, Analysis, and Writing the manuscript

Alexander G. Levshin: Provided technical advice and guidance throughout the research process

Simon G. Teklay: Offered review and editing services for the manuscript, Enhancing clarity

References

1. Ale, M. O., Manuwa, S. I., & Olukunle. (2023). Effect of Forward Speed and Drive Wheel on the Performance of a Semi-Automatic Cassava Planter. *Achievers Journal of Scientific Research*, 4(2), 85-94.
2. AMIA. (2021). Nardi Dora Air Drill| AMIA. Retrieved 15 December 2023, from AMIA Online Shop website: <https://www.agrimarketia.com/product/nardi-dora-air-drill>
3. Badua, S. A., Sharda, A., Strasser, R., & Ciampitti, I. (2021). Ground speed and planter downforce influence on corn seed spacing and depth. *Precision Agriculture*, 22(4), 1154-1170. <https://doi.org/10.1007/s11119-020-09775-7>
4. Benos, L., Tsaopoulos, D., & Bochtis, D. (2020). A Review on Ergonomics in Agriculture. Part I: Manual Operations. *Applied Sciences*, 10(6), 1905. <https://doi.org/10.3390/APP10061905>
5. Biocca, M., Fanigliulo, R., Grilli, R., Benigni, S., Fornaciari, L., & Pochi, D. (2022). Effect of sowing speed and width on spacing uniformity of precision seed drills effect of sowing speed and width on spacing uniformity of precision seed drills. *INMATEH - Agricultural Engineering*, 66(1), 9-18. <https://doi.org/10.35633/inmateh-66-01>
6. Brandelero, E. M., Adami, P. F., Modolo, A. J., Baesso, M. M., & Fabian, A. J. (2015). Seeder performance under different speeds and its relation to soybean cultivars yield. *Journal of Agronomy*, 14(3), 139-145. <https://doi.org/10.3923/ja.2015.139.145>
7. Demetriou, D., See, L., & Stillwell, J. (2013). A parcel shape index for use in land consolidation planning. *Transactions in GIS*, 17(6), 861-882. <https://doi.org/10.1111/j.1467-9671.2012.01371.x>
8. Diao, X., Takeshima, H., & Zhang, X. (2020). *An Evolving Agricultural Paradigm of Mechanization Development: How Much Can Africa Learn from Asia?*
9. Griffel, L. M., Vazhnik, V., Hartley, D., Hansen, J. K., & Richard, T. L. (2018). Machinery maneuvering efficiency and perennial crops: Field shape complexity defines the efficiency. *ASABE 2018 Annual International Meeting*. American Society of Agricultural and Biological Engineers. <https://doi.org/10.13031/aim.201800440>
10. Herodowicz-Mleczak, K., Piekarczyk, J., Kaźmierowski, C., Nowosad, J., & Mleczak, M.

- (2022). Estimating soil surface roughness with models based on the information about tillage practises and soil parameters. *Journal of Advances in Modeling Earth Systems*, 14(3). <https://doi.org/10.1029/2021MS002578>
11. Ivančan, S., Sito, S., & Fabijanić, G. (2004). Effect of precision drill operating speed on the intra-row seed distribution for parsley. *Biosystems Engineering*, 89(3), 373-376. <https://doi.org/10.1016/j.biosystemseng.2004.07.007>
 12. Janulevičius, A., Šarauskis, E., Čiplienė, A., & Juostas, A. (2019). Estimation of farm tractor performance as a function of time efficiency during ploughing in fields of different sizes. *Biosystems Engineering*, 179, 80-93. <https://doi.org/10.1016/j.biosystemseng.2019.01.004>
 13. Khater, M. M. I. (2017). Designing a software to calculate the field capacity for full mechanized agriculture practices in light soils. *Misr Journal of Agricultural Engineering*, 34(3), 1143-1154.
 14. Kirkegaard Nielsen, S., Munkholm, L. J., Lamandé, M., Nørremark, M., Edwards, G. T. C., & Green, O. (2018). Seed drill depth control system for precision seeding. *Computers and Electronics in Agriculture*, 144, 174-180. <https://doi.org/10.1016/j.compag.2017.12.008>
 15. Matsuura, S. (2023). Bayes estimator of process capability index Cpk with a specified prior mean. *Communications in Statistics - Theory and Methods*, 52(7), 2215-2227. <https://doi.org/10.1080/03610926.2021.1947508>
 16. Montgomery, D. C. (2013). *Introduction to Statistical Quality Control* (Seventh Edition). New York City: Wiley.
 17. Oksanen, T. (2013). Shape-describing indices for agricultural field plots and their relationship to operational efficiency. *Computers and Electronics in Agriculture*, 98, 252-259. <https://doi.org/10.1016/j.compag.2013.08.014>
 18. Shinde, G. U., Mandal, S., Ghosh, P. K., Bhalerao, S., Kakade, O., Motapalukula, J., & Das, A. (2023). Farm Mechanization. In P. K. Ghosh, A. Das, R. Saxena, K. Banerjee, G. Kar, & D. Vijay (Eds.), *Trajectory of 75 years of Indian Agriculture after Independence* (pp. 475–496). Singapore: Springer Nature Singapore. https://doi.org/10.1007/978-981-19-7997-2_18
 19. Srivastava, A., Goering, C., & Rohrbach, R. (2006). *Engineering principles of agricultural machines* (second; Peg McCann, Ed.). American Society of Agricultural and Biological Engineers.
 20. Toba, A. L., Griffel, L. M., & Hartley, D. S. (2020). Devs based modeling and simulation of agricultural machinery movement. *Computers and Electronics in Agriculture*, 177(August). <https://doi.org/10.1016/j.compag.2020.105669>
 21. Toscano, P., Cutini, M., Filisetti, A., Premoli, E., Porcu, M., Catalano, N., ..., & Brambilla, M. (2022). Workability Assessment of Different Stony Soils by Soil–Planter Interface Noise and Acceleration Measurement. *AgriEngineering*, 4(4), 1139-1152. <https://doi.org/10.3390/agriengineering4040070>
 22. Vereshchagin, N. I., Levshin, A. G., Skorokhodov, A. N., Kiselyov, S. N., Kosyrev, V. P., Zubkov, V. V., & Gorshkov, M. I. (2018). *Organization and technology of mechanized work in crop production* (12th ed.). Moscow.
 23. Wang, Y., Zhang, W., Luo, X., Zang, Y., Ma, L., Zhang, W., ..., & Zeng, S. (2024). Effect of Vibration Conditions on the Seed Suction Performance of an Air-Suction Precision Seeder for Small Seeds. *Agriculture*, 14(4), 559. <https://doi.org/10.3390/AGRICULTURE14040559>
 24. Wu, C. W., Pearn, W. L., & Kotz, S. (2009). An overview of theory and practice on process capability indices for quality assurance. *International Journal of Production Economics*, 117(2), 338-359. <https://doi.org/10.1016/j.ijpe.2008.11.008>
 25. Zangiev, A. A., & Skorokhodov, A. N. (2018). *Practical on the operation of the machine and tractor fleet [Electronic resource]: textbook. handbook*. St. Petersburg: Lan, Electron. dan.

تأثیر ویژگی‌های مزرعه بر عملکرد بذرکار پنوماتیک: مطالعه موردی در اریتره

ت. آ. مدهن^۱، آ. ج. لوشین^۲، س. ج. تکلا^۱

تاریخ دریافت: ۱۴۰۳/۰۷/۰۶

تاریخ پذیرش: ۱۴۰۳/۰۸/۱۵

چکیده

استفاده کارآمد از ماشین‌های کشاورزی به‌طور قابل توجهی کمیت و کیفیت عملیات زراعی را بهبود می‌بخشد؛ بنابراین، بهینه‌سازی سرعت و زمان عملیات زراعی ضروری است. عواملی مانند شکل هندسی مزرعه و زبری (زمختی) سطح خاک (SSR) به‌طور قابل توجهی بر عملکرد بذرکار تأثیر می‌گذارند. هدف این تحقیق، ارزیابی چگونگی تأثیر این عوامل کلیدی بر عملکرد بذرکار بود: (۱) اندازه و شکل مزرعه و (۲) اثرات متقابل سرعت کارنده و زبری سطح خاک (SSR). شاخص‌های عملکردی، ظرفیت مزرعه‌ای مؤثر (F_{eff})، کارایی (η) و سرعت متوسط کارنده (V_a)، با استفاده از نرم‌افزار SAS تحلیل شدند. شاخص‌های تحذب (I_{con}) و درجه مستطیل شکل بودن (I_R) هر قطعه با استفاده از ابزار مدیریت داده حداقل هندسه محصور ArcGIS محاسبه شد، در حالی که انحراف استاندارد ارتفاع (σ_e) با استفاده از پایتون محاسبه شد. مقادیر به‌دست‌آمده برای F_{eff} ، η و V_a به مقدار زیادی متغیر بودند و به‌ترتیب با مقادیر در محدوده ۱۰/۲ تا ۳/۱ هکتار در ساعت، ۳۰٪ تا ۶۵/۷٪ و ۵/۲ تا ۱۷ کیلومتر در ساعت به‌دست آمد. شاخص قابلیت پردازش V_a (Cpk) 0.22 نشان‌دهنده‌ی چالش قابل توجهی در تحقق محدودیت‌های تعیین شده است. با افزایش طول مسیر قطعه، ظرفیت مزرعه‌ای مؤثر نیز افزایش یافت ($R^2=42\%$)، در حالی که با افزایش نسبت محیط به مساحت (P/A) کاهش یافت ($R^2=51\%$). علاوه بر این، با افزایش شاخص‌های I_{con} و I_R ظرفیت مزرعه‌ای مؤثر روند افزایشی نشان داد، در حالی که با افزایش ضریب فشردگی (I_{com}) و شاخص مربعی (I_{sp}) کاهش یافت؛ اگرچه این روابط از نظر آماری معنادار نبودند. سطوح بالاتر زبری عموماً منجر به کاهش η می‌شدند. علاوه بر این، کارکرد بذرکار با سرعت بالاتر در زمین ناهموار منجر به کاهش قابل توجهی در کارایی شد. بنابراین، طراحی مجدد قطعات زمین برای به حداقل رساندن دشواری‌های مرزی آن‌ها، از بین بردن ناهنجاری‌های توپوگرافی و اجرای رویه‌های پیش‌کاشت ویژه هر قطعه، به‌طور قابل توجهی عملکرد بذرکار را بهبود خواهد بخشید.

واژه‌های کلیدی: زبری سطح خاک، شاخص شکل و اندازه، ظرفیت مزرعه‌ای مؤثر، قطعات زمین

۱- گروه مهندسی کشاورزی، دانشکده مهندسی و تکنولوژی، مای-نفی، اریتره

۲- دانشگاه دولتی کشاورزی روسیه، آکادمی کشاورزی تیمیریازف مسکو، مسکو

(*)- نویسنده مسئول: (Email: noahtesas@gmail.com)